2-2007

Fragmentation of methyl chloride studied by partial positive and negative ion yield spectroscopy

D. Ceolin
Uppsala University

Maria Novella Piancastelli
Uppsala University, maria-novella.piancastelli@physics.uu.se

Renaud Guillemin
CNRS, Laboratoire de Chimie Physique-Matière et Rayonnement

Wayne C. Stolte
University of Nevada, Las Vegas, wcstolte@lbl.gov

S-W Yu
Lawrence Berkeley National Laboratory

See next page for additional authors

Fragmentation of methyl chloride studied by partial positive and negative ion-yield spectroscopy

D. Céolin, M. N. Piancastelli, R. Guillemin, W. C. Stolte, S.-W. Yu et al.

Citation: J. Chem. Phys. **126**, 084309 (2007); doi: 10.1063/1.2464093
View online: http://dx.doi.org/10.1063/1.2464093
View Table of Contents: http://jcp.aip.org/resource/1/JCPSA6/v126/i8
Published by the American Institute of Physics.

Fragmentation of methyl chloride studied by partial positive and negative ion-yield spectroscopy

D. Céolin and M. N. Piancastelli
Department of Physics, Uppsala University, P.O. Box 530, SE-75121 Uppsala, Sweden

R. Guillemin
Department of Chemistry, University of Nevada, Las Vegas, Nevada 89154-4003
and Laboratoire de Chimie Physique-Matiere et Rayonnement, UMR 7614, 11 rue Pierre et Marie Curie, 75231 Paris Cedex 05, France

W. C. Stolte
Department of Chemistry, University of Nevada, Las Vegas, Nevada 89154-4003
and Advanced Light Source, Lawrence Berkeley National Laboratory, Berkeley, California 94720

S.-W. Yu
Department of Chemistry, University of Nevada, Las Vegas, Nevada 89154-4003
and Center for X-Ray Optics, Lawrence Berkeley National Laboratory, Berkeley, California 94720

O. Hemmers and D. W. Lindle
Department of Chemistry, University of Nevada, Las Vegas, Nevada 89154-4003

(Received 27 January 2006; accepted 9 January 2007; published online 28 February 2007)

The authors present partial-ion-yield experiments on the methyl chloride molecule excited in the vicinity of the Cl2*p* and C1*s* inner shells. A large number of fragments, cations produced by dissociation or recombination processes, as well as anionic species, have been detected. Although the spectra exhibit different intensity distributions depending on the core-excited atom, general observations include strong site-selective fragmentation along the C–Cl bond axis and a strong intensity dependence of transitions involving Rydberg series on fragment size. © *2007 American Institute of Physics*. [DOI: 10.1063/1.2464093]

I. INTRODUCTION

Resonant excitation or ionization of a core electron by a photon in the soft-x-ray regime promotes a molecule to a rather unstable potential energy surface. The excited system relaxes on a very short time scale, typically tens of femtoseconds or less, most likely by emitting an electron(s), then adopting a different geometry and/or breaking one or several chemical bonds. Below the core-level ionization limits, electronic relaxation processes lead generally to singly charged ions, produced either by participator or spectator resonant Auger decay. Above the core-level ionization limits, the intermediate state is itself singly charged and relaxes preferentially by normal Auger decay, leading to doubly charged species. In rarer situations, emission of several electrons during the (resonant or not) Auger decay is possible. In each case, ion fragmentation is dependent on internal energy, i.e., upon the electronic and vibrational energies stored in the system: the more energy stored, the more the ion is likely to dissociate. These phenomena can be highlighted by detection of one or several emitted particles. High-resolution electron spectroscopy is a suitable tool to study the ultrafast processes of electronic and nuclear rearrangements, whereas ion spectroscopy typically monitors processes taking place on longer time scales. However, one can obtain a wealth of information on dynamics of core-excited species by analysis of partial-ion-yield spectra, as demonstrated in experiments showing unusual fragmentation products formed by recombination processes. For example, in the case of H_2O excited along the resonance $O1s \rightarrow 2b_2$, Piancastelli *et al.*[1] measured the production of the H_2^+ ion dependent on the way the intermediate state is prepared. The maximum intensity for H_2^+ production is detected following the decay of higher vibrational levels of the intermediate state, i.e., when the molecule undergoes large-amplitude bending and stretching vibrations. This recombination process probed by ion spectroscopy is an illustration of a fast nuclear motion occurring on the same time scale as electronic relaxation. Monitoring one particular ion fragment over a large photon-energy range allows one to emphasize transitions usually hidden (when ions are not selected by mass and charge) by one or several electronic states with higher absorption cross section. The most striking example is the observation by anion spectroscopy of doubly excited states usually concealed by shape resonances above the ionization thresholds of the C1*s* and O1*s* core orbitals of CO,[2] of the two nonequivalent N1*s* orbitals of N_2O,[3] and of the O1*s* orbital of CO_2.[4]

We report here a partial-ion-yield study of CH_3Cl excited around the C1*s* and Cl2*p* thresholds. Fragmentation of methyl chloride excited around the Cl2*p* edge has been investigated previously using charge-separation mass spectrometry and photoelectron-photoion coincidence,[5] yielding accurate information at four distinct photon energies. A general overview of the different transitions around the C1*s* edge has been described in Refs. 6 and 7 by inner-shell electron-energy-loss studies, without giving details on disso-

ciation of the molecule. In our measurements, we have taken advantage of the tunability of synchrotron radiation over a wide energy range, and of partial-ion-yield measurements, to follow the production of each charged species—positive or negative—with an excitation resolution less than the core-hole-lifetime broadening.

A key experimental finding from this study is the confirmation of the observations of Piancastelli *et al.*[8] of high fragmentation efficiency when exciting ethylene and acetylene compounds along core-to-Rydberg series. Such excited molecular species with one electron in an orbital far from the ionic core relaxes preferentially by spectator-Auger decay, and the singly charged ion, with two valence holes and one electron in a diffuse outer orbital, remains in a highly excited state more susceptible to dissociation. These results have been established at both the Cl2*p* and C1*s* edges. A second finding is the strong selective fragmentation along the C–Cl bond after promotion of a carbon *K*-shell electron to the first empty orbital, as particularly seen along the CH_iCl^{++} series ($i=0-3$), where a (quasi-) complete suppression of the $8a_1$ excited state is observed, and along the CH_i^+ series, which is strongly enhanced. Such selectivity is a signature of the localization of the electron vacancies in the final state along the C–Cl bond with subsequent bond rupture.

II. EXPERIMENT

Experiments were performed on beamline 8.0.1.3 at the Advanced Light Source, Lawrence Berkeley National Laboratory. The monochromator resolution achieved at 204 eV photon energy was estimated as 30 meV, using previous measurements of the $4s(^3D)^2D_{5/2}$ atomic chlorine transition at 204.31 eV with a theoretical lifetime broadening of 5.3 meV.[9] The resolution at $h\nu=300$ eV was estimated as 70 meV based on previous measurements of CO.[2] Ion mass and charge characterization was done with a 180° hemispherical analyzer with a resolution of 1 mass in 50.[10] Briefly, the fragments are created by interaction with the light beam at the exit of an effusive gas jet. Ions are extracted from the gas cell by an electric field and focused on the entrance slit of the analyzer by an electrostatic lens. They are then deflected between the plates of the analyzer and refocused onto the exit slit before being detected by a channel electron multiplier. The potentials of the analyzer electrodes can be tuned and/or switched in polarity to select fragments with a specific mass and charge. The working pressure in the target chamber was set to 1×10^{-5} Torr, and the chamber was isolated from the beamline vacuum by differential pumping. Due to the relative natural abundance of ^{35}Cl and ^{37}Cl isotopes in a 3:1 ratio, some pairs of ionic fragments are not discernible in the measurements, namely, $CH_3^{35}Cl^+$ and $CH^{37}Cl^+$, $CH_2^{35}Cl^+$ and $C^{37}Cl^+$, as well as their doubly charged counterparts.

III. RESULTS AND DISCUSSION

We present in Fig. 1 the partial ion yields of the Cl^+ and C^+ ions recorded over a photon-energy range large enough to cover both the Cl2*p* and C1*s* edges. The intensity of the transitions located below (above) the Cl2*p* ionization thresholds is weak (strong) compared to the ones located just below (above) the C1*s* threshold, quasi-independently of the fragment. In the vicinity of the carbon *K* edge, the large background is attributed mainly to contributions of ions coming from relaxation of Cl2*p* core holes.

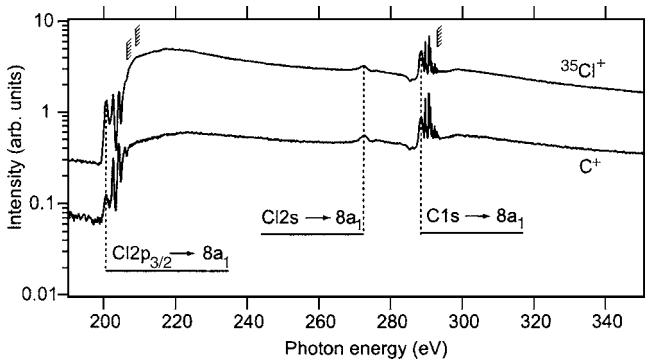

FIG. 1. Partial ion yields of the C^+ and $^{35}Cl^+$ fragments taken over a large photon-energy range including the Cl2*p*, Cl2*s*, and C1*s* edges.

A. Cl2*p* edge

Excitation of methyl chloride around the Cl2*p* edges leads to a large number of cations: CH_iCl^+ and CH_iCl^{++} for both $^{35}Cl^+$ and $^{37}Cl^+$ isotopes, CH_i^+ with $i=0-3$, C^{++}, CH_2^{++}, $^{35}Cl^+$, $^{37}Cl^+$, $^{35}Cl^{++}$, $^{35}Cl^{+++}$, H^+, H_2^+, H_3^+, $H^{35}Cl^+$, $H^{35}Cl^{++}$, and two anions $^{35}Cl^-$ and C^-. Table I provides the peak assignments in the 198–280 eV photon-energy range. The energy position of the $8a_1$ transition given in Ref. 5 was used for energy calibration.

In Fig. 2, we present the partial ion yields for the CH_iCl^+ series. Assignments for the five resonant features are as follows. The lowest-lying resonance (A) is attributed to the $Cl2p_{3/2}\rightarrow 8a_1$ transition and its large width (870 meV full width at half maximum) is due to its strong repulsive character. In addition to elongation of the C–Cl bond, this tran-

TABLE I. Energy positions and assignments of lines observed in the region of the Cl2*p* and Cl2*s* ionization thresholds. Peak labels refer to Fig. 2.

	Energy (eV)		Assignment	
Label	This work	Ref. 5	$Cl2p_{3/2}\rightarrow$	$Cl2p_{1/2}\rightarrow$
A	200.70	200.70	$8a_1$	···
···	202.35	···	···	$8a_1$
B	202.55	202.50	$4s$	···
C	204.25	204.10	$4p$	$4s$
D	205.25	···	$5s$	···
E	206	···	···	$4p$
···	206.31	206.26	IP	···
F	206.90	···	···	$5s$
···	207.96	207.90	···	IP[a]
	Position (eV)		Attribution	
Extra peaks[b]	This work	Ref. 6	$Cl2s\rightarrow$	
···	272.60	271.70	$8a_1$	
···	276.60	···	Rydberg	

[a]Deduced from the spin-orbit splitting value.
[b]Cf. Fig. 1.

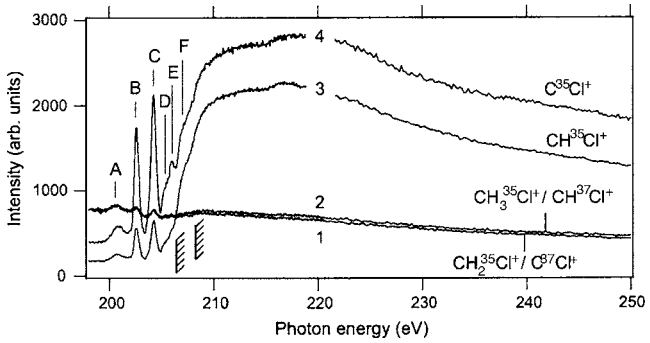

FIG. 2. Partial ion yields of the CH_iCl^+ fragments ($i=0-3$) around the Cl2p ionization thresholds. Labels refer to Table I.

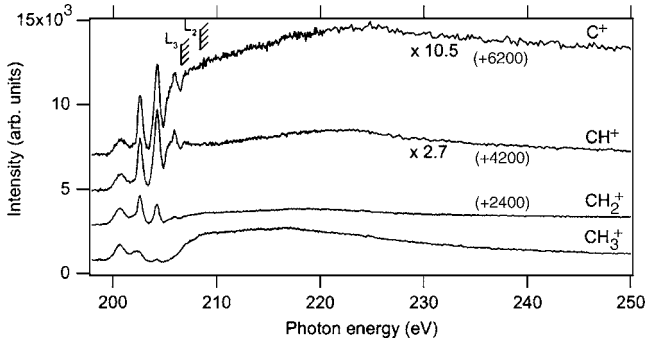

FIG. 3. Partial ion yields of the CH_i^+ fragments ($i=0-3$) around the Cl2p ionization thresholds. Spectra are normalized to the intensity of the first peak (Cl2$p_{3/2} \rightarrow 8a_1$). Scaling factors and offsets on the vertical axis are shown. Positions of the Cl2$p_{3/2}$ and Cl2$p_{1/2}$ ionization potentials are indicated by L_3 and L_2, respectively.

sition to a core-excited state may have influence on the population of vibrational levels corresponding to stretching and bending motions in the methyl group. With photoelectron photoion coincidence measurements, Thissen *et al.*[5] assigned unresolved structures on this resonance to a population of excited vibrational states separated by 250 meV and corresponding to the C–H stretching mode. We also observe such structures for a large number of fragments ($CHCl^+$, CCl^+, and CH_i^+, $i=0-3$, especially); however, their intensity and energy spacing do not allow us to suggest an attribution to specific vibrational modes (bending and/or stretching). The second peak (B) at 202.5 eV is a superposition of the Cl2$p_{1/2} \rightarrow 8a_1$ transition and the Cl2$p_{3/2} \rightarrow 4s$ Rydberg transition. This assignment is confirmed by the CH_3^+ yield (see below). At higher energies, the Rydberg series (peaks C–F) corresponds to a sequential overlap of the transitions Cl2$p_{3/2}$ and 2$p_{1/2}$ to empty orbitals of 4s, 4p, 5s, and 5p atomic characters.

In Fig. 2, curves 1 and 2 are associated with the $CH_2^{35}Cl^+/C^{37}Cl^+$ and $CH_3^{35}Cl^+/CH^{37}Cl^+$ fragments, respectively, whereas curves 3 and 4 correspond to $CH^{35}Cl^+$ and $C^{35}Cl^+$, respectively. For the first two, weak features at resonances A–C sit on a high decreasing background attributed to direct valence photoemission. In contrast, the $CH^{35}Cl^+$ and $C^{35}Cl^+$ ions are much more abundant around the Cl2p edges. For these latter fragments, the Cl2$p \rightarrow 8a_1$ transition and transitions to the first two Rydberg orbitals are clearly resolved. In addition, for CCl^+ only, three additional transitions, one resolved peak (E) and two shoulders (D and F), are also visible. Above threshold, a large structure dominates curves 3 and 4, with two distinct maxima depending on the ion. Precise assignment remains difficult because doubly excited states generally overlap the shape resonances in this region;[2,4] such an overlap could be the origin of these intensity variations above threshold.

Figure 3 shows partial ion yields for the CH_i^+ ions ($i=0-3$). With the exception of the methyl ion, the Cl2$p \rightarrow 4s$, 4p, and 5s Rydberg excitations are well resolved. Weak production of CH_3^+ following excitation to the lower Rydberg components allows us to assign the two lowest-lying spectral features to the Cl2$p_{3/2} \rightarrow 8a_1$ and Cl2$p_{1/2} \rightarrow 8a_1$ transitions, with an intensity ratio of 2:1 in the absence of exchange effects. With an experimental resolution of 30 meV, we measured a spin-orbit splitting of 1.65 eV, in very good agreement with the value of 1.64 eV obtained in x-ray photoelectron spectroscopy studies by Aitken *et al.*[11]

Below threshold, the main experimental finding for both the CH_iCl^+ and the CH_i^+ series is the relative intensity enhancement of the spectral structures corresponding to Rydberg transitions as the fragments become lighter, as already observed by Piancastelli *et al.* for ethylene/acetylene compounds[8] and by Stolte *et al.* for water.[12] The explanation is that a core-to-Rydberg excited molecule is more likely to relax by spectator-Auger decay: the excited electron is far from the nucleus and the system relaxes preferentially by emitting an electron from an orbital having strong overlap with the core hole, i.e., a valence orbital, while the initially excited electron remains as a "spectator." The resulting ion is still in an excited state and is energetically more likely to dissociate. Above threshold, we observe an equivalent tendency: the lighter the fragment, the larger the relative intensity. The position of the maxima above threshold, however, depends on the fragment mass in the CH_i^+ series: for lighter fragments, the maximum is shifted towards higher energies (the maxima positions are 216.6, 218.85, 222.8, and 225 eV for CH_3^+, CH_2^+, CH^+, and C^+, respectively). We speculate that as the photon energy increases above threshold, more vibrational and/or electronic energy is stored in the singly charged intermediate state. After Auger decay, this energy stays in the system as internal energy, supporting subsequent dissociation.

In Fig. 4, we compare the ion production for the CH_iCl^{++} series. The Cl2$p_{1/2,3/2} \rightarrow 8a_1$ resonances and the Rydberg series have very weak intensities and sit on a low background. Of course, the production of doubly charged species in the below-threshold region is not expected, and their formation must be due to many-electron processes. The CH_3Cl^{++}, CH_2Cl^{++}, and $CHCl^{++}$ spectra are very similar in shape, with a strong intensity increase above the Cl2p edges due to the opening of electronic relaxation by Auger effect. With the exception of the CCl^{++} spectrum, the lighter the fragment, the more abundant its production. Also, the higher production of $CHCl^{++}$ relative to the three other dications supports the work of Wong *et al.*,[13] who predicted its stability in a linear geometry. We also note that the spectral shapes for $CHCl^+$ and $CHCl^{++}$ are very similar above threshold. One

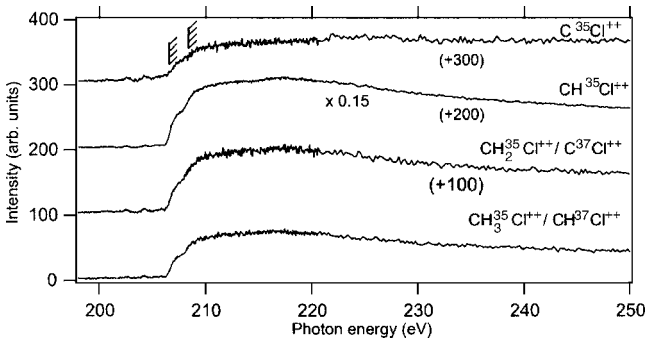

FIG. 4. Partial ion yields of the CH_iCl^{++} fragments (i=0–3) around the Cl2p ionization thresholds. A scaling factor and offsets on the vertical axis are shown.

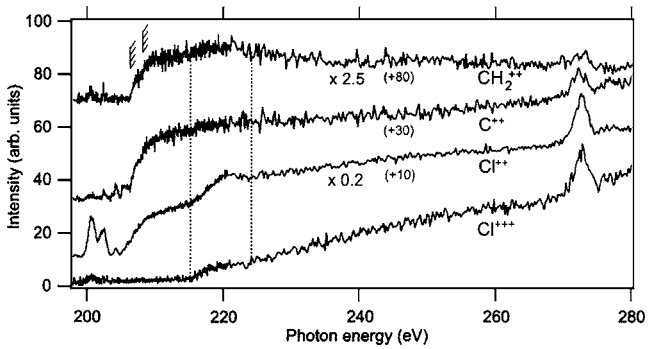

FIG. 6. Comparison of $^{35}Cl^{+++}$, $^{35}Cl^{++}$, C^{++}, and CH_2^{++} ions yields. The dotted lines delimit a zone corresponding to the opening of dissociation pathways involving triply charged species. Scaling factors and offsets on the vertical axis are shown.

explanation could be an equivalence of how they are produced, with the location of the positive charges at the time of the dissociation being the only difference,

$$CH_3Cl + h\nu \rightarrow CH_3Cl^{+*} + e^-,$$

$$CH_3Cl^{+*} \rightarrow CHCl^+ + H^+ + H \text{ or } CHCl^{++} + 2H + e^-.$$

In contrast, the CCl^{++} spectrum differs completely from CCl^+, both above and below thresholds. We attribute this behavior to an instability of the CCl^{++} dication due to Coulombic repulsion.

For the Cl^{++} spectrum shown in Fig. 5, there is a large contribution from below-threshold resonances that cannot be explained by anion-cation pair production: the only detected anions are C^- and Cl^-, and C^- intensity is much too weak. The production of Cl^{++} in the 199–206 eV photon-energy range can occur via several processes. Thissen *et al.*[5] suggested the possibility of electronic relaxation in core-excited chlorine atoms produced after ultrafast dissociation. An ultrafast process is supported by the fact that a transition of an electron from the Cl2p orbital to the lowest unoccupied molecular orbital leads to the core-equivalent system CH_3Ar, which is repulsive along the C–Ar bond. The fragmentation leads to a neutral CH_3 and an excited chlorine atom that relaxes primarily to Cl^+, with minority production of Cl^{++} via multielectron processes. These observations are consistent with the results in Figs. 2 and 4, where the intensity of the $8a_1$ resonance is weak across both the singly charged and doubly charged CH_iCl series. However, we note that shake-off processes can accompany Auger decay, also leading to doubly charged ions below threshold likely to dissociate. Some possible pathways for formation of doubly charged chlorine are

$$CH_3Cl + h\nu \rightarrow CH_3Cl^*,$$

$$CH_3Cl^* \rightarrow CH_3Cl^{+*} + e^- \text{ (resonant Auger decay)}$$

$$(CH_3)^* + Cl^{+*} + e^- \text{ (dissociation)}$$

$$(CH_3)^* + Cl^{++} + 2e^- \text{ (second-step electronic relaxation),}$$

$$\rightarrow CH_3Cl^{++} + 2e^- \text{ (resonant Auger decay + shake off)}$$

$$(CH_3)^* + Cl^{++} + 2e^- \text{ (and dissociation),}$$

$$\rightarrow (CH_3)^* + Cl^* \text{ (ultrafast dissociation)}$$

$$(CH_3)^* + Cl^{++} + 2e^- \text{ (resonant Auger decay and shake off).}$$

Brackets for the CH_3 groups indicate a possible dissociation process, before, after, or on a time scale comparable to electronic relaxation. The notation " *" corresponds to a true, or, with brackets, to a possible electronic excitation. At variance with the observation of Thissen *et al.*, production of Cl^{++} increases slightly above threshold with the opening of Auger decay.

Production of Cl^{+++} ion is negligible below threshold. In Fig. 6, we show measurements at higher photon energies for the cations Cl^{+++}, Cl^{++}, C^{++}, and CH_2^{++}. The production threshold of Cl^{+++} does not coincide with that of Cl^{++} and is shifted to higher energy (above $h\nu$=215.6 eV). One explanation could be that the formation of the triply charged ion requires a shake-up process during Cl2p ionization. This double-electron process (one core ionization + one valence-electron excitation) must lead, after normal Auger decay, to a molecule or chlorine atom (in the case of ultrafast fragmentation) in an unstable highly excited electronic state that autoionizes to form a triply charged ion. If the shake-up process does not produce intermediate states energetic enough, only doubly charged species will be formed, as seen below

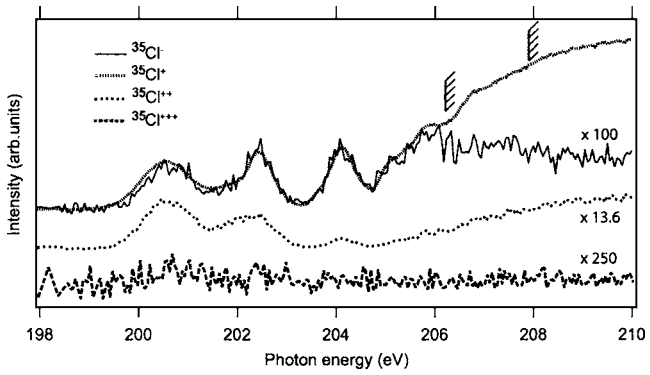

FIG. 5. Qualitative comparison of partial ion yields of the $^{35}Cl^-$, $^{35}Cl^+$, $^{35}Cl^{++}$, and $^{35}Cl^{+++}$ fragments below the Cl2p ionization thresholds. Scaling factors are used to normalize the spectra to the intensity of the first transition.

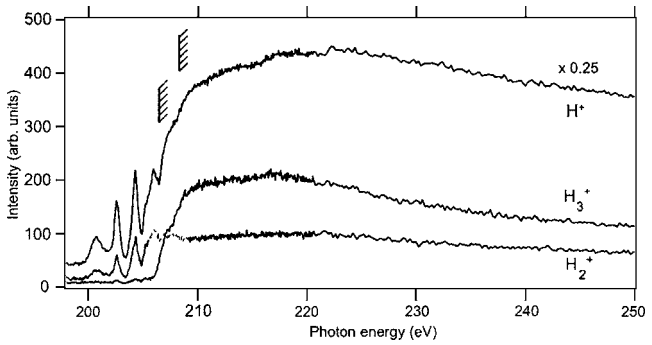

FIG. 7. Partial ion yields of H^+, H_2^+, and H_3^+ fragments in the region of the Cl2*p* ionization thresholds. A scaling factor for H^+ is used for clarity.

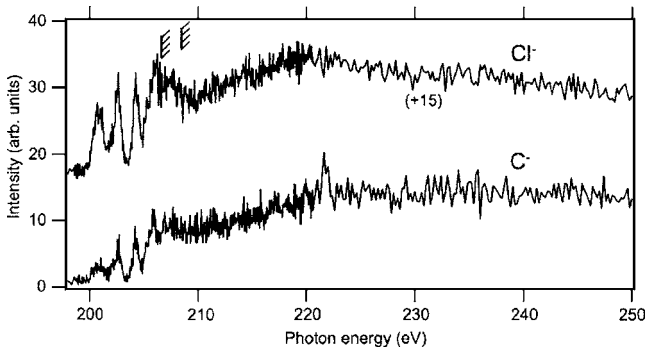

FIG. 9. Partial ion yields of the two detectable anions, $^{35}Cl^-$ and C^-, in the region of the Cl2*p* ionization thresholds. For clarity an offset is used on the vertical axis for Cl^-.

$h\nu$=215.6 eV. This explanation is supported by the presence around 220 eV photon energy (in Fig. 6, the region delimited by dotted lines) of an intensity bump for several fragments [Cl^{++}, Cl^+, CH_i^+ (i=0–3), or CH_i^{++} (i=0 or 2)] and can be assigned to fragmentation of doubly excited states that may lead to triply charged species. In the doubly charged chlorine-ion spectrum, this bump is attributed to the opening of dissociation paths leading to $CH_3^{+(*)}+Cl^{++}$, in competition with the paths $CH_3Cl+h\nu$ ($\geqslant$215.6 eV)$\rightarrow CH_3^{(*)}+Cl^{+++}$, with the methyl groups in both cases susceptible to dissociation. Similarly, the path $CH_3Cl+h\nu \rightarrow CH_i^{++(*)}+Cl^+$ must be open as well, but the only relevant doubly charged species we are able to detect are C^{++} and CH_2^{++}. In the C^{++}, CH_2^{++}, and Cl^+ spectra, the bump around 220 eV photon energy (also seen in the CH_i^+ series in Fig. 3) is present but weaker than for the couples Cl^{+++}/CH_i and Cl^{++}/CH_i^+.

In Fig. 7, we show the H^+, H_2^+, and H_3^+ ion yields. Below threshold, the formation of H^+ and H_2^+ on the $8a_1$ resonance is relatively important, whereas it is virtually nonexistent for H_3^+. However, the production of the latter is slightly visible over the Rydberg series, where the two other ions are clearly present. Above threshold, production of all three ions increases and reaches maxima around 220 eV. The maximum peak positions of the $8a_1$ and Rydberg resonances do not differ with photon energy for all three ions, in contrast to the observations in H_2O excited along the $O1s \rightarrow 2b_2$ resonance,[1] where maximum production of H_2^+ shifted slightly towards the high-energy side of the resonance, i.e., towards higher vibrational levels presumably inducing formation of molecular hydrogen. In the current results, no narrowing of the H_2^+ or H_3^+ resonance peaks compared to H^+ has been found either, also in contrast to the observations of Piancastelli *et al.* on acetylene,[8] where the explanation was that the intermediate core-excited state leads to production of recombination fragments only when higher vibrational levels are excited.

Figure 8 displays the measured HCl^+ and HCl^{++} ion yields. The observation of these two ions is surprising because their formation requires three distinct steps: breaking of a H–C bond, creation of a H–Cl bond, and breaking of the Cl–C bond. Though we cannot determine the order of these processes from our measurements (the formation mechanisms of these species will be described in a forthcoming paper[14]), it is worth noting that the HCl^+ and HCl^{++} spectra show different behaviors compared to the Cl^+ and Cl^{++} yields, respectively. The main difference between Cl^+ and HCl^+ is an intensity decrease of the latter above the Cl2*p* ionization limit compared with the resonant region. In contrast, the HCl^{++} mimics perfectly the Cl^{++} yield. Thus, HCl^+ and HCl^{++} seem to arise from two distinct processes, or chains of processes.

In Fig. 9, we show the partial ion yields of the two detectable anions. Both Cl^- and C^- are present below and above thresholds, but no clear structure which could be related to doubly excited states, as described by Stolte *et al.* in other molecules,[2] is evident. Comparison with anions collected after excitation around the C *K* edge is given in the next section.

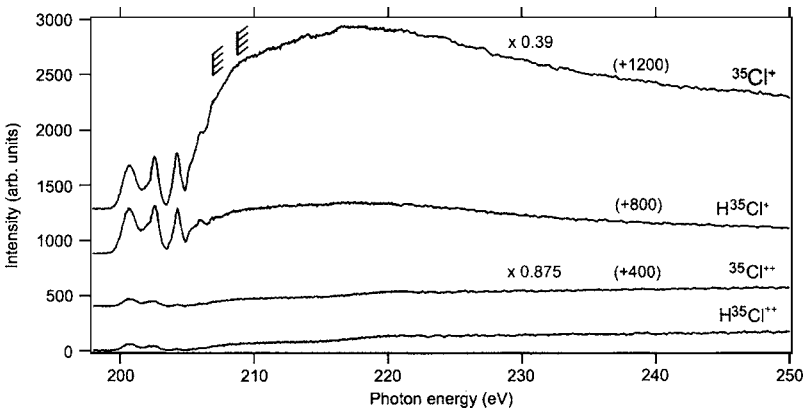

FIG. 8. Partial ion yields of the $^{35}Cl^+$, $H^{35}Cl^+$, $^{35}Cl^{++}$, and $H^{35}Cl^{++}$ fragments around the Cl2*p* ionization thresholds. The spectra are normalized to the intensity of the $Cl2p_{3/2} \rightarrow 8a_1$ transition. Scaling factors and offsets on the vertical axis are shown.

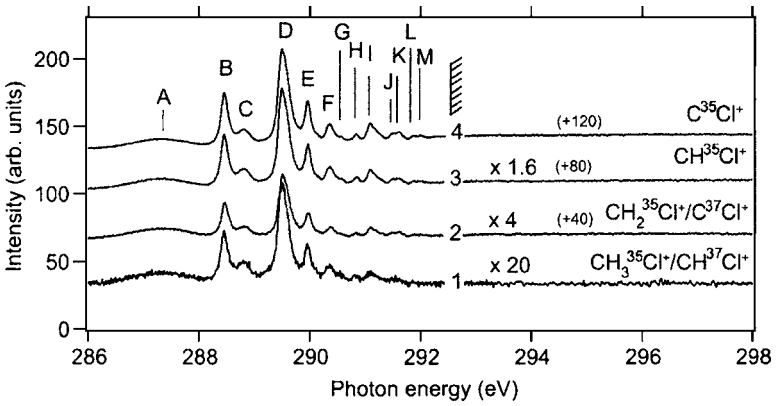

FIG. 10. Partial ion yields of the CH_iCl^+ fragments ($i=0-3$) around the C1*s* ionization threshold. Spectra are normalized to the intensity of the first peak ($C1s \rightarrow 8a_1$). Scaling factors and offsets on the vertical axis are shown. Labels refer to Table II.

B. C1*s* edge

Excitation of methyl chloride around the carbon K edge also leads to a large number of cations: CH_iCl^+, CH_iCl^{++}, $CH_i^+(i=0-3)$, H^+, H_2^+, H_3^+, Cl^+, Cl^{++}, Cl^{+++}, HCl^+, HCl^{++}, and C^{++}, as well as three anions: Cl^-, C^-, and H^-.

The partial ion yields for the series $CH_iCl^+(i=0-3)$ in the region of the C1*s* ionization threshold are shown in Fig. 10. A large number of features are observed on a high background due to Cl2*p* ionization (see Fig. 1). Assignments of the C *K*-edge peaks by Hitchcock and Brion, based on the intermolecular correlation method of Robin[15,16] is presented in Ref. 6 and 7. This method correlates the term values, i.e., peak energies relative to the ionization potential of the core orbital, to specific atomiclike orbital symmetries $(s,p,d,\ldots)$. The first intense transition is attributed to the promotion of a C1*s* electron to the $8a_1$ antibonding orbital. The narrower peaks at higher energy are attributed to a Rydberg progression, with vibrational substructures for some states (see Table II). Spectra 1 and 2 in Fig. 10 correspond to a 1:3 mixture of the ions $CH^{37}Cl^+/CH_3^{35}Cl^+$ and $C^{37}Cl^+/CH_2^{35}Cl^+$, respectively, whereas spectra 3 and 4 correspond only to the fragments $CH^{35}Cl^+$ and $C^{35}Cl^+$, respectively. By normalizing to the intensity of the $8a_1$ resonance, we observe very similar spectra, contrary to results in the Cl2*p* region (see Fig. 2); formation of the ions in this series apparently ensues from very similar dissociation processes.

The shapes of the ion-yield spectra for the CH_i^+ series in Fig. 11 are quite different from the CH_iCl^+ series in Fig. 10. The intensity of the $8a_1$ resonance is comparable to the intensities in the Rydberg series; this is most significant for CH_3^+. As for other series, the lighter the fragment, the higher the intensity of the Rydberg peaks. For C^+ and CH^+, the peak progression extends more clearly to higher photon energy than for CH_2^+ and the methyl parent ion. The strong intensity of the lowest-energy resonance for these ions is evidence of the C–Cl bond rupture following decay to final states with electron vacancies localized near the C–Cl bond.

In Fig. 12, the spectra represent production of doubly charged CH_iCl ions ($i=0-3$). The main observation is the near-total suppression of the $8a_1$ resonance in all the spectra, again clear evidence that promotion of a core electron to the $8a_1$ orbital leads to an unstable species likely to dissociate along the C–Cl bond. In addition, due to Coulomb repulsion, dications fragment more easily than singly charged ions, lowering the intensity of the entire Rydberg series. We note also an intensity increase for CCl^{++} at the C1*s* threshold, corresponding to opening of electronic relaxation via Auger decay. The different spectral shapes of CH_iCl^+ and CH_iCl^{++} show that the formation of the dictations cannot be consid-

TABLE II. Energy positions and assignments of peaks observed after excitation around the C1*s* orbital of methyl chloride. Notations are from Refs. 6 and 7, where the Rydberg levels are treated as extensions of the halogen atomic orbitals. According to these last two references, nomenclature reflecting molecular symmetries a_1 and e in the C_{3v} group has been retained for some Rydberg states, contrary to assignments presented in Table I.

	Position (eV)		
Label	This work	Refs. 6 and 7	Attribution C1*s*→
A	287.34	287.34	$8a_1$(C–Cl)
B	288.45	288.34	$4sa_1$
C	288.79	288.54	$8a_1$(C–H)/$4sa_1+\nu_{CH}$
D	289.50	289.39	$4pe$
E	289.95	289.78	$4pe+\nu_{CH}$
F	290.37	290.19	$4pa_1/4pe+2\nu_{CH}$
G	290.56	⋯	
H	290.83	⋯	
I	291.08	290.94	$5pe$, $4d$
J	291.46	291.34	$5pa_1$
K	291.60	⋯	
L	291.87	⋯	
M	292.01	⋯	
⋯	292.40	⋯	IP C1*s*

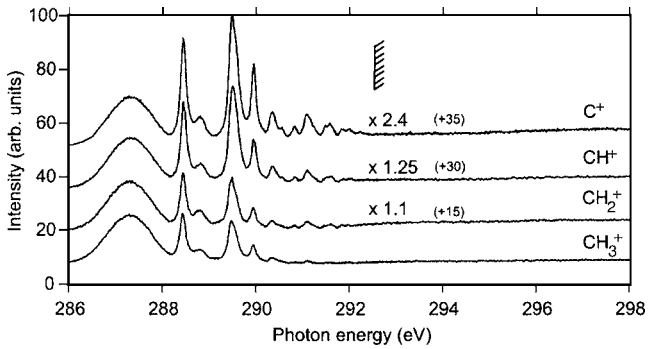

FIG. 11. Partial ion yields of the CH_i^+ fragments ($i=0-3$) around the C1*s* ionization threshold. Spectra are normalized to the intensity of the first peak ($C1s \rightarrow 8a_1$). Scaling factors and offsets on the vertical axis are shown.

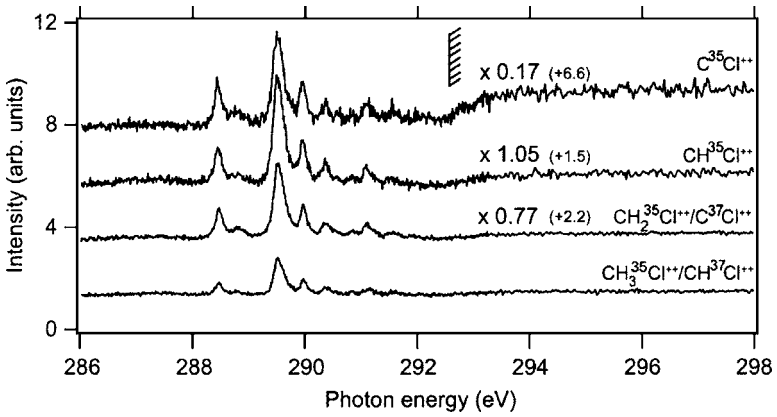

FIG. 12. Partial ion yields of the CH_iCl^{++} fragments (i=0–3) around the C1s ionization threshold. Spectra are normalized to the intensity of the first peak (C1s $\rightarrow 8a_1$). Scaling factors and offsets on the vertical axis are shown.

ered as a second step following formation of the singly charged ions. Rather, doubly charged species can be formed directly when the energy content of the core-excited intermediate state is high enough for it to decay to final states with two valence holes, i.e., above the double-ionization threshold. The subsequent fragmentation probabilities seem to be essentially the same in the Rydberg region for all doubly charged species, at variance with the relative intensity increase of the Rydberg series for lighter fragments observed in the singly charged series (see Figs. 2, 3, 10, and 11).

As seen in Fig. 13, the intensity distribution of the H_2^+ and H_3^+ fragments following C1s core excitation is quite similar to the one for H^+. Below threshold, the $8a_1$ orbital and the Rydberg series are clearly resolved in the case of H_2^+ formation, whereas for H_3^+, due to a lower yield, only the most intense peaks are well resolved. As observed around the Cl2p threshold, no shift in energy or narrowing of peaks is observed for the two recombination fragments, as compared with H^+. This means that the vibrational population of the intermediate state does not affect production of these ions (see discussion of Fig. 7). One interesting point is the suppression of the H_2^+ and H_3^+ formations above the C1s threshold; the opposite behavior was observed for the Cl2p threshold.

The fragments $H^{35}Cl^+$ and $H^{35}Cl^{++}$ were also observed (not shown), mainly below the C1s threshold. However, the associated spectra mimic the ones of $^{35}Cl^+$ and $^{35}Cl^{++}$, strongly suggesting that their formation is due to the post-photodissociation collision between atomic or ionic chlorine and hydrogen rather than a direct combination process induced by core excitation.

In Fig. 14, we show the partial ion yields for the anions detected near the C1s threshold, namely, C^-, $^{35}Cl^-$, and H^-. As in the case of Cl2p excitation/ionization, the $8a_1$ resonance and the Rydberg series show somewhat different spectral intensities compared to the cation of the same mass. The main difference between the anion yields around the C1s and Cl2p thresholds (Fig. 9) is their relatively strong intensity above the Cl2p threshold. A possible explanation for above-threshold anion production would be the presence of doubly excited states, as observed in several other systems;[2–4] but in the present case there is no clear resonant structure, just a relatively broad distribution of intensity. To explain this observation, we suggest that above threshold the dominant process is normal Auger decay following core-level ionization. Although anion production due to fragmentation of dications generated by Auger decay is probably very weak, it can oc-

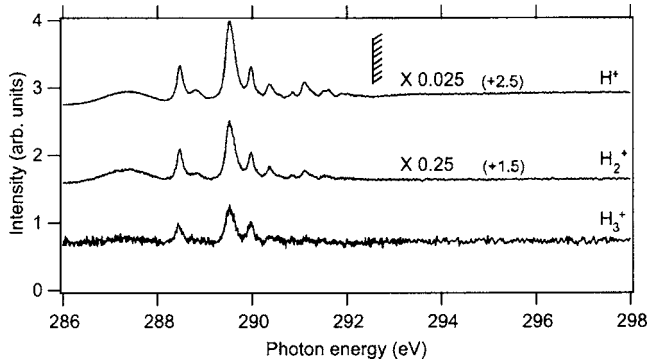

FIG. 13. Partial ion yields of the H^+, H_2^+, and H_3^+ fragments in the region of the C1s ionization threshold. Scaling factors and offsets on the vertical axis are shown.

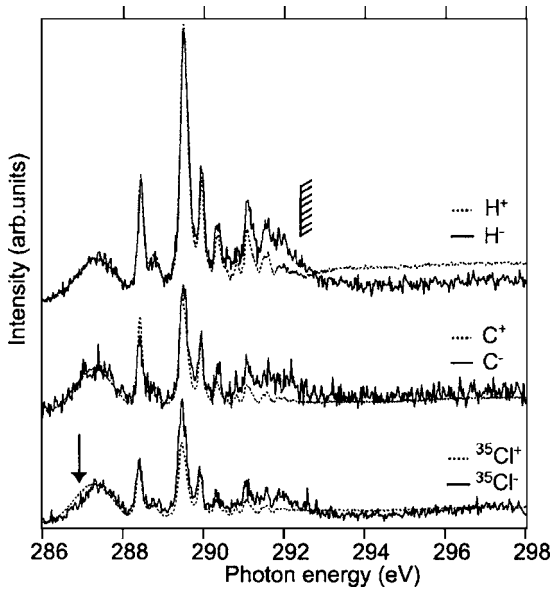

FIG. 14. Partial ion yields of the detectable anions C^-, $^{35}Cl^-$, and H^- fragments around the C1s ionization threshold. These spectra are compared to partial ion yields of C^+, $^{35}Cl^+$, and H^+ normalized to the intensity of the C1$s \rightarrow 8a_1$ resonance and calibrated in energy at the first Rydberg component. As described in the text, the arrow indicates the zone corresponding to shorter C–Cl bond distances.

cur for a polyatomic system such as CH_3Cl, if three positive charges can be accommodated in the fragmentation process, such as

$$CH_3Cl^{++} \rightarrow C^+ + 2H^+ + H + Cl^-.$$

At variance with this, anion production from a molecular trication is extremely unlikely, because it would be necessary to distribute four positive charges over a relatively small number of fragments. Therefore, a possible explanation for the different anion behaviors around the two edges is that deeper C1*s* core holes are more likely to undergo Auger-cascade or double-Auger processes leading to triply or multiply charged species relative to shallower Cl2*p* holes, implying a negligible probability for anion formation.

Finally, H^- is formed after photoexcitation in the C1*s* region, but not near the Cl2*p* edge. This can be compared with results on SF_6 (Ref. 17) and CH_3OH (Ref. 18) for which the number of different anions is larger for the case of inner-shell excitation of the central sulfur or carbon atoms, respectively, than for the case of inner-shell excitation of the peripheral fluorine or oxygen atoms. In sulfur hexafluoride, this behavior is attributed to the presence of a potential barrier due to the electronegativity difference between the central and peripheral atoms temporarily trapping the emitted electron. The explanation for site-specific production of H^- in methanol, or methyl chloride, is less straightforward. One possibility could be related to proximity or steric hindrance; the ejected electron may have a higher probability to be captured by free hydrogen in the cases of emission from the carbon rather than from the oxygen or chlorine atoms. Also, comparison of the intensity distribution of anion spectra after C1*s* ionization with spectra of the same mass cations shows a lower intensity on the left side of the C1$s \rightarrow 8a_1$ resonance for Cl^-, in contrast to the other anions (see Fig. 14). This could mean that core-level photoexcitation preferentially reaches the Franck-Condon region corresponding to longer (shorter) C–Cl bond distances at lower (higher) photon energies along the profile of this strongly antibonding resonance, suggesting a possible bond-length dependence in the formation of an anionic species.

IV. CONCLUSION

We have measured the partial ion yields following excitation of the CH_3Cl molecule in the region of the Cl2*p* and C1*s* core-level thresholds. We confirm the role of Rydberg transitions in the formation of lighter fragment species and the strong localization of the electron vacancies in the final state along the C–Cl bond after promotion of a carbon *K*-shell electron to the first empty orbital. Furthermore, some remarkable effects have been observed, such as anion production, dependent on the environment of the initially excited atom, namely, whether its location in the molecule is central or peripheral, as well as a possible bond-length dependence on the formation of Cl^-.

ACKNOWLEDGMENTS

The authors thank the staff of the ALS for their excellent support. Support from the National Science Foundation under NSF Grant No. PHY-01-40375 is gratefully acknowledged. The authors particularly thank Professor J. A. R. Samson for the use of the instrument used in this research. This work was performed at the Advanced Light Source, which is supported by DOE (DE-AC03-76SF00098).

[1] M. N. Piancastelli, A. Hempelmann, F. Heiser, O. Gessner, A. Rudel, and U. Becker, Phys. Rev. A **59**, 300 (1999).
[2] W. C. Stolte, D. L. Hansen, M. N. Piancastelli, I. Dominguez-Lopez, A. Rizvi, O. Hemmers, H. Wang, A. S. Schlachter, M. S. Lubell, and D. W. Lindle, Phys. Rev. Lett. **86**, 4504 (2001).
[3] S.-W. Yu, W. C. Stolte, G. Öhrwall, R. Guillemin, M. N. Piancastelli, and D. W. Lindle, J. Phys. B **36**, 1255 (2003).
[4] G. Öhrwall, M. M. Sant'Anna, W. C. Stolte, I. Dominguez-Lopez, L. T. N. Dang, A. S. Schlachter, and D. W. Lindle, J. Phys. B **35**, 4543 (2002).
[5] R. Thissen, M. Simon, and M.-J. Hubin-Franskin, J. Chem. Phys. **101**, 7548 (1994).
[6] A. P. Hitchcock and C. E. Brion, J. Electron Spectrosc. Relat. Phenom. **13**, 193 (1978).
[7] A. P. Hitchcock and C. E. Brion, J. Electron Spectrosc. Relat. Phenom. **14**, 417 (1978).
[8] M. N. Piancastelli, W. C. Stolte, G. Öhrwall, S.-W. Yu, D. Bull, K. Lantz, A. S. Schlachter, and D. W. Lindle, J. Chem. Phys. **117**, 8264 (2002).
[9] M. Martins, J. Phys. B **34**, 1321 (2001).
[10] W. C. Stolte, Y. Lu, J. A. R. Samson, O. Hemmers, D. L. Hansen, S. B. Whitfield, H. Wang, P. Glans, and D. W. Lindle, J. Phys. B **30**, 4489 (1997).
[11] E. J. Aitken, M. K. Bahl, K. D. Bomben, J. K. Gimzewski, G. S. Nolan, and T. D. Thomas, J. Am. Chem. Soc. **102**, 4873 (1980).
[12] W. C. Stolte, M. M. Sant'Anna, G. Öhrwall, I. Dominguez-Lopez, M. N. Piancastelli, and D. W. Lindle, Phys. Rev. A **68**, 022701 (2003).
[13] M. W. Wong, B. F. Yates, R. H. Nobes, and L. Radom, J. Am. Chem. Soc. **109**, 3181 (1987).
[14] C. Miron, International Workshop on Photoionization (IWP2005), Campinas, Brazil, 2005 (unpublished); C. Miron, P. Morin, D. Céolin, L. Journel, and M. Simon, Phys. Rev. Lett. (submitted).
[15] M. B. Robin, Int. J. Quantum Chem. **6**, 257 (1972).
[16] M. B. Robin, *Higher Excited States of Polyatomic Molecules* (Academic, New York, 1974), Vol. 1.
[17] M. N. Piancastelli, W. C. Stolte, R. Guillemin, A. Wolska, S.-W. Yu, M. M. Sant'Anna, and D. W. Lindle, J. Chem. Phys. **122**, 94312 (2002).
[18] W. C. Stolte, G. Öhrwall, M. M. Sant'Anna, I. Dominguez-Lopez, L. T. N. Dang, M. N. Piancastelli, and D. W. Lindle, J. Phys. B **35**, 253 (2005).